Published in final edited form as:
*Exp Eye Res*. 2012 May ; 98: 88–96.

# Preservation of retinotopic map in retinal degeneration

**John Xie**[a,*], **Gene-Jack Wang**[b], **Lindy Yow**[a], **Mark S. Humayun**[a], **James D. Weiland**[a], **Carlos J. Cela**[c], **Hossein Jadvar**[a], **Gianluca Lazzi**[c], **Elona Dhrami-Gavazi**[d], and **Stephen H. Tsang**[d]

[a]Doheny Eye Institute, University of Southern California, 1355 San Pablo St., DVRC-100, Los Angeles, CA 90033, USA

[b]Medical Department, Brookhaven National Laboratory, Upton, NY, USA

[c]Department of Electrical and Computer Engineering, University of Utah, Salt Lake City, UT, USA

[d]Bernard & Shirlee Brown Glaucoma Laboratory, Edward S. Harkness Eye Institute, Columbia University Medical Center, New York, NY, USA

## Abstract

Retinal degenerations trigger the loss of photoreceptors and cause the remaining de-afferented neural retina to undergo remodeling. Concerns over this potential retinal synaptic reorganization following visual loss have raised questions regarding the usefulness of visual restoration via retinal electrical stimulation. We have used quantitative positron emission tomography (PET) and 2-deoxy-2-[$^{18}$F]fluoro-D-glucose (FDG) to objectively evaluate the connection between the retina and the primary visual cortex under both light and transcorneal electrical stimulation (TcES) in five subjects with retinal degeneration (RD) who have had more than ten years of light-perception-only best visual acuity and five age-matched normal-sighted controls. All subjects underwent quantitative PET with FDG as the metabolic tracer during stimulation of the right eye under both light stimulation condition and transcorneal electrical stimulation (TcES) using ERG-Jet contact lens electrode. Cortical activation maps from each stimulation condition were obtained using statistical parametric mapping. TcES phosphene threshold current and qualitative visual cortex activation from both stimulation conditions were compared between the two subject groups. Average phosphene threshold current was 0.72 ± 0.18 mA for the five normal-sighted controls and 3.08 ± 2.01 mA for the retinal degenerative subjects. Phosphene threshold current was significantly higher in retinal degenerative subjects compared to normal-sighted controls ($p < 0.05$). We found both light stimulation and TcES resulted in retinotopically mapped primary visual cortex activation in both groups. In addition, the patterns of early visual area activation between



*Corresponding author. Tel.: +1 626 297 3055; fax: +1 626 614 8006. john.jianxie@gmail.com (J. Xie).

**disclosures**

*Financial Disclosures*: All the authors listed have no financial interest related to the research work being submitted.

*Contributions to Authors*: Design of the study (JX, GW, LY, MH, JW, HJ); Conduct of the study (JX, GW, LY, CC, GL, ED, ST); Collection of the data (JX, GW, ED, CC); Management, analysis, and interpretation of the data (JX, GW, CC); Preparation, review, or approval of the manuscript (JX, GW, MH, JW, HJ).

*Statement about Conformity with Author Information*: IRB approval was prospective. The submitted study obtained IRB approval from the Health Science Institutional Review Board at the University of Southern California, the Committee on Research Involving Humans Subjects (CORIHS) at Stony Brook State University, and the Human Subject Institutional Review Board at Columbia University.

the two subject groups are more similar during TcES than light stimulation. Our findings suggest primary visual cortex continues to maintain its retinotopy in RD subjects despite prolonged visual loss.

**Keywords**

2-deoxy-2-[$^{18}$F]fluoro-$_{D}$-glucose; positron emission tomography; transcorneal electrical stimulation; retinal degeneration; primary visual cortex; retinotopic map

## 1. Introduction

Retinal degenerative diseases are clinically and genetically heterogeneous group of primary retinal degeneration in which abnormalities of the photoreceptors (rods and cones) or the retinal pigment epithelium lead to progressive visual loss (Hartong et al., 2006; Sharma and Ehinger, 1999). Although the course and progression of the diseases show considerable variation between individuals, they are typically characterized by initial symptoms of night blindness, with onset in adolescence or early adulthood, loss of peripheral vision and, as the disease progresses, loss of central vision leading to complete blindness or severe visual impairment. Currently there is no cure for retinal degenerative diseases.

Although the symptoms, severity and progression may vary between different outer retinal degenerative conditions, one common finding is the loss of photoreceptors. Postmortem evaluations of the retina in subjects with retinitis pigmentosa (RP), the predominant form of retinal degenerative disease, have shown that a large number of cells remain in the inner retina compared with the outer retina (Humayun et al., 1999a; Santos et al., 1997; Stone et al., 1992). In severe RP, only 4% of photoreceptors remained in the macula, but 80% of the inner retina and 30% of ganglion cells were preserved. In extra-macular regions, only 40% of inner retina remained. Thus by cell counting, the inner retina in RP appears to be less affected by the disease compared with the photoreceptors.

Furthermore, direct electrical stimulation of the retina in humans with RP results in light perception (phosphenes), supporting the idea that some neural elements exist even in end stage degeneration (Humayun et al., 1999b; Rizzo et al., 2003). Studies using computational phenotyping, however, suggest that the inner retina undergoes significant remodeling during retinal degeneration (Marc et al., 2003; Marc and Jones, 2003). This type of remodeling may lead to disruption of spatial cell patterning and impede rescue strategies using retinal prosthetic implants, photoreceptor transplants or stem cell therapies, which all depend on a viable, intact retinal circuitry following photoreceptor degeneration.

Since the first demonstration by Potts et al. (1968) that subjective phosphene sensation and visual cortical response can be evoked by an electrical current passing through the cornea, a number of studies have been conducted to determine the site of retinal stimulation (Kawamura, 1986; Potts and Inoue, 1970; Shimazu et al., 1999; Takei, 1988). Findings from both human and animal studies have indicated that the neural elements activated by electrical stimulation are located in the inner retinal layers, more proximal than the photoreceptors. Several groups have used transcorneal electrical stimulation (TcES) to

estimate the residual function of Inner retinal cells by means of threshold current necessary to evoke phosphenes in RP subjects (Fujikado et al., 2007; Gekeler et al., 2006; Morimoto et al., 2006; Potts and Inoue, 1969). It was demonstrated that the threshold current needed to evoke phosphene in RP subjects was significantly higher than in normal-sighted controls. More recently, the use of electrically evoked response has been utilized as a pre-operative screening tool for retinal prosthesis clinical trials (Humayun et al., 1996; Yanai et al., 2003). When conventional means of assessing vision fails to elicit light perception due to loss of photoreceptors in retinal degenerative (RD) subjects with bare or no light perception, the function of the remaining viable inner retinal layers can still be evaluated electrically by passing a current through the retina.

Functional imaging studies have demonstrated that a light stimulus can elicit visual cortex activation in subjects with severe outer retinal degeneration. Case studies, however, have shown the patterns of brain activation differ from normal-sighted controls due to both visual impairment and potential neural remodeling following visual loss (Baker et al., 2005; Dilks et al., 2009). The use of a light stimulus in RD subjects requires functional photoreceptors for signal transduction to the brain, which may not reflect the full extent of synaptic connection between the viable inner retinal layers and the visual cortex. To elucidate this functional connection, objective measures that can directly demonstrate activation of the primary visual cortex in response to inner retinal layer stimulation are necessary. To date, no functional imaging study has been carried out to look at the brain response to retinal electrical stimulation. In this study, we present the brain activation results from both light and transcorneal electrical stimulation in normal-sighted and RD subjects using quantitative positron emission tomography (PET) coupled with metabolic tracer 2-deoxy-2-[$^{18}$F]fluoro-$_{D}$-glucose ($^{18}$FDG).

## 2. Materials & methods

### 2.1. Retinal degenerative subjects

Five right-handed subjects with primary retinal degeneration (mean age: 43.7 ± 10.5 yrs) were recruited for the study from Columbia University (Table 1). The human experiments were conducted at Brookhaven National Laboratory, and the study was approved by the Human Subject Institutional Review Board at Columbia University, Committee on Research Involving Humans Subjects (CORIHS) at Stony Brook State University, and the Health Science Institutional Review Board (HSIRB) at the University of Southern California. All subjects have had at least ten years of light perception or near light-perception visual acuity at the time of the study and met stringent inclusion/exclusion criteria including but not limited to age range between 18 and 80 years; must exhibit primary retinal dystrophy as diagnosed by a certified ophthalmologist; no major acute or chronic medical illness that may affect brain function; no significant life-threatening health problem such as seizure or congestive heart failure; no uncontrolled diabetes mellitus with blood glucose exceeding 180 mg/dL on any day of the study; not pregnant; no use of psychiatric medication that can affect brain function; no other significant ocular disease besides primary retinal degeneration. To minimize potential confounding factors, the subjects all had early-onset visual loss occurring before adulthood. The location and extent of remaining vision at the

time of PET study varied between the five subjects: RD 1 reported seeing best in the right mid peripheral visual field of her right eye; RD 2 reported losing mostly central vision with preservation of peripheral sight; RD 3 reported light-perception vision in a pinhole hear the central visual field of his right eye; Both RD 4 and 5 reported severe loss of peripheral vision with more preservation of central vision. RD 2 appeared to have the best remaining vision in the group and RD 4 the worst.

DNA testing was conducted at Columbia University Medical Center and the results are shown in (Table 1). DNA was extracted from whole blood with the QIAamp DNA Blood Maxi Kit 51194 (Diagen Inc., Valencia, CA, USA). One subject had a novel c.710delT frameshift mutation in the gene encoding *CRX*, and a second had a G172S mutation in the gene encoding *ABCA4*. The remaining three subjects were screened with the ARRP APEX recessive array (Asper Biotech, Inc., Tartu, Estonia). No RP-associated mutations were detected by the array screening.

Optical coherence tomography (OCT) study conducted using Stratus OCT 3000 (Carl Zeiss Meditec, Dublin, CA, USA) on the RD subjects showed loss of retinal thickness due primarily to loss of photoreceptors in the outer nuclear layer while the retinal nerve fiber layer was preserved. The OCT results for RD 1 –4 are shown in (Fig. 1).

### 2.2. Normal-sighted controls

Five normal-sighted, right-handed, age-matched human subjects (mean age: 34.7 ± 10 years) without any history of vision loss or neurologic disease were enrolled in the study (Table 1). The human experiments were conducted at Brookhaven National Laboratory with the approval from both CORIHS and HSIRB.

### 2.3. TcES setup

A clinical grade DS7A neurostimulator (Digitimer LTD, Hertfordshire, England) was used to generate stimulus pulses for TcES (Fig. 2). The stimulator, capable of generating alternating polarity current pulses, is connected to a contact lens corneal electrode via a D185-HB4 output cable (Digitimer, LTD). Stimulus pulse trains were generated using DG2A trigger generator, which connected to the stimulator for continuous electrical stimulation. During the experiment, the neurostimulator was set to output a continuous train of alternating current pulses consisted of repeating cathodic pulse followed by an anodic pulse; each current pulse had 2-ms pulse duration; alternating pulses are generated at 2 Hz with inter-pulse interval of 996 ms.

### 2.4. Corneal electrode

ERG-Jet (Fabrinal SA, La Chaux-de-Fonds, Switzerland) corneal electrode was used for TcES. This is a disposable monopolar hard contact lens electrode approved by the FDA for human use. The electrode contains a thin circular gold foil overlaid on top of the concave surface of the poly(methylmethacrylate) contact lens (Fig. 2). The circular geometry of the gold contact matches the circular symmetry of the eye and makes this electrode well suited for delivering electrical current evenly to the eye. The return electrode, placed on the right temporal skin, was an adhesive backed pregelled, silver–silver/chloride electrode (24”

Button Snap, Integra NeuroSupplies, Plainsboro, NJ, USA) with an impedance of approximately 800 Ω over the frequency range of the stimulus pulse used in TcES.

### 2.5. Phosphene threshold determination

Phosphene threshold was defined as the stimulation current amplitude, at which 50% of the presented current pulses were correctly detected by the subject during TcES. Since cathodic current pulse elicited slightly brighter phosphene than anodic pulses as reported by the subjects, the phosphene threshold was determined using the cathodic current pulse. Two psychophysical methods were combined to arrive at the threshold. First, a reference electrical stimulus (0.5 mA, 2-ms pulse width at 2 Hz) was presented, and the subject was asked whether or not a phosphene was perceived. The current level was adjusted up or down according to the "method of limits" to quickly approximate threshold. This threshold was then used in a second step to generate a short stimulus pulse train (8–10 pulses in length). The subject was instructed to count only the visually perceptible pulses. Fine adjustment on the current was made to arrive at the final threshold, in which 50% of the pulses in the pulse train were perceived as phosphenes.

### 2.6. Baseline study protocol

Baseline study served as a reference in subtraction statistical analysis for both light stimulation and TcES. Subjects were first dark-adapted by sitting inside a completely darkened room while wearing a blindfold for 30 min; then, they remained blindfolded following $^{18}$FDG injection and throughout the 30-min $^{18}$FDG radiotracer uptake phase.

### 2.7. Light stimulation protocol

Subjects were first dark-adapted for 30 min as described in the baseline study protocol prior to $^{18}$FDG injection. During light stimulation, the subject's chin was comfortably placed on a modified slit-lamp chin rest and the right eye was exposed to a flashing light stimulus from a CRT computer monitor during the 30-min $^{18}$FDG uptake phase. The left eye remained blindfolded. To ensure comfort and avoid adaptation, the light stimulus was turned off for 30 s after every 5 min of stimulation. The light stimulus program was run from a Dell OptiPlex model GX1 266 MHz desktop computer and displayed on a Viewsonic OptiQuest Model Q71 17-inch CRT monitor. The photic stimulus, which subtended central 10° field of view on the retina, was a repeating sequence (30-s duration) of a flashing white square with temporal frequency increasing incrementally from 2 to 30 Hz. The average photopic illuminance of the light stimulus, measured with IL1700 Research Radiometer (International Light, Inc, Newburyport, MA, USA) coupled to a SED033 detector (International Light, Inc.), was 1.76 lumen·m$^{-2}$. To ensure proper eye fixation, a high-definition video camera recorded the pupillary light reflection throughout the light stimulation study.

### 2.8. TcES protocol

Corneal examination of the right eye was performed at the beginning and at the end of each study to rule out corneal abrasion caused by the corneal electrode. The exam was done using fluorescein strips (Flu-Glo, Akorn Pharmaceuticals, Decatur, IL, USA) and Mag-Lite flashlight fitted with #47 Blue Tricolor Gel filter (B&H Photo-Video-Pro-Audio, New York,

NY, USA) to mimic emission spectrum of cobalt blue filter. Two drops of tetracaine topical anesthetic (0.5% Tetravisc, OCuSOFT, Inc, Richmond, TX, USA) was first instilled in the right eye to minimize any stinging sensation from the fluorescein dye. Surface corneal images were captured using Olympus digital camera (Model C-5050, Olympus, Optical Co., LTD, Center Valley, PA, USA). The concave cup of the ERG-Jet electrode was filled with lidocaine gel (3.5% Akten, Akorn, Pharmaceuticals, Decatur, IL, USA) before it was placed on the subject's right eye. After phosphene threshold was determined, subject was seated in a completely darkened room with eyes blindfolded for the 30-min dark adaptation. This was immediately followed by TcES with a continuous train of rectangular, monophasic, alternating polarity current pulses (2 Hz, 2-ms pulse width, 1.5 × phosphene threshold current amplitude) was delivered to the electrode during the 30-min $^{18}$FDG uptake phase. To make the subject comfortable during the study, the stimulator was turned off for 30 s after every 5 min of continuous stimulation.

### 2.9. PET imaging

PET scans were acquired on a whole-body, high-resolution positron emission tomography (SiemensTI ECAT HR+; with 4.6 mm × 4.6 mm × 4.2 mm resolution at the center of the field of view and 63 slices) in 3-D dynamic acquisition mode using $^{18}$FDG. The methods for quantitative PET brain imaging are summarized in the paper published by Wang (Wang et al., 1993).

### 2.10. Statistical analysis

Differences in measures of regional brain glucose metabolism during light stimulation and TcES were evaluated using Statistical Parametric Mapping (SPM 5, Wellcome Trust Center for Neuroimaging, University College London, London, UK). Each PET image was resliced and normalized into ICBM 152 standard brain anatomy space, and then analyzed using paired *t*-test to search for voxels with increased brain $^{18}$FDG activity (activation) during either light stimulation or TcES compared to baseline. The resultant SPM map was a group average of five subjects from each stimulation condition.

## 3. Results

### 3.1. Subjective sensation during light stimulation

The central projection of the square photic stimulus during light stimulation resulted in perception of a well-delineated white flashing square in the central 10° field of view of the right eye for all the normal controls. RD subjects generally perceived a diffuse, white flashing light from their right eye. The quality of the light sensation was described as "cloudy." RD1 reported seeing the light best in her right mid peripheral visual field; RD2 reported seeing a circular rim of flashing light around his mid periphery; RD3 reported pulsing light the size of a pinhead in the center of his visual field; and both RD4 and RD5 reported seeing the light stimulus in their central visual field. On a scale of 1–10 ('10' being the brightest light the subject had ever seen), they gave a rating between 5 and 6 for the light stimulus.

### 3.2. Phosphene threshold

The average threshold current for ERG-Jet corneal electrode was 0.72 ± 0.18 mA for the five normal-sighted controls and 3.08 ± 2.01 mA for the RD subjects (Table 1). Phosphene threshold current was significantly higher in RD subjects compared to normal controls ($p$ = 0.031, two sample $t$-test).

### 3.3. Subjective phosphene sensation during TcES

During TcES with the ERG-Jet electrode, all five normal-sighted subjects consistently reported a semilunate, crescent-shaped white phosphene in the peripheral temporal visual field of the right eye that extended between the superior and inferior limits of the visual field (Fig. 3). The phosphene was akin to the rapid closing of a camera shutter, with brightness rated between 4 and 5 on a scale of 1–10. The alternating monophasic current pulses resulted in perception of alternating phosphene intensity with the cathodic pulse reported to be brighter than the anodic pulse.

RD subjects were asked to describe the shape and size of the phosphene by touching a piece of Play-Doh kneaded into a circular torus to represent their visual field (Fig. 3). All five RD subjects perceived phosphene in their right peripheral visual field during TcES, although there was some variation in reported phosphene shape and size (Fig. 3). The phosphene was reported to be faint and rapid, but readily perceived. On a subjective intensity scale of 1–10, the RD subjects rated the phosphene between 2 and 3. Four subjects (RD 1, 2, 3, and 5) also noted streak-like radiation of the phosphene emanating from the location of highest intensity to along the right visual periphery towards the center of the visual field. They also reported seeing the brightest phosphene immediately after the stimulator was turned on, and the intensity gradually faded with subsequent electrical pulses, but remained perceptible. Like the normal controls, cathodic current pulse was perceived to be brighter than anodic pulse.

### 3.4. Light stimulation PET

Regions of increased brain activity during light stimulation were determined by subtracting normalized light stimulation PET image from the baseline PET image and performing parametric statistical analysis. Statistically significant voxels ($p < 0.05$), averaged across five normal controls or five RD subjects, were plotted on the SPM maps. For normal controls, light stimulation activated primary visual cortex (Brodmann area 17, abbreviated as BA 17) bilaterally at the posterior occipital pole (Figs. 4 and 5). Activation was found to be both above and below the calcarine sulcus, which has been shown to process visual input from the macula. Occipital pole activation was more extensive on the right than the left hemisphere (Fig. 5). In addition, there was a significant region of activation in the anterior calcarine cortex on the left hemisphere above the calcarine sulcus (Fig. 5, top row, blue arrowhead). Activation in this region of the occipital cortex is consistent with studies that looked at monocular photic stimulation in humans (Miki et al., 2000; Rombouts et al., 1996; Toosy et al., 2001). There was also bilateral activation of secondary visual cortex (BA 18) and activation of left association visual area (BA 19).

Light stimulation in the RD subjects activated primary visual cortex (BA 17) in the right occipital pole and secondary visual cortices (BA 18 and 19) on the left hemisphere.

Comparing to normal controls, a smaller region of activation in the right occipital pole reached statistical significance in the RD group. This can be explained by differences in the extent and location of visual loss among the RD subjects.

In addition to visual cortex, significant activation in bilateral orbitofrontal and prefrontal cortex was observed in both normal-sighted and RD subjects (Fig. 4). These cortical areas have been shown to play a role in visual attention and fixation (Anderson et al., 1994; de Haan et al., 2008).

### 3.5. TcES PET

Regions of increased brain activity during TcES were determined by subtracting TcES PET image from the baseline PET image and performing a parametric statistical analysis. Statistically significant voxels ($p < 0.05$) were plotted on the SPM maps (Figs. 4 and 5).

For normal controls, TcES with ERG-Jet stimulation resulted in statistically significant activation of a region in the anterior primary visual cortex (BA 17) on the left hemisphere (Fig. 5, second row, blue arrowhead). This region of the primary visual cortex processes visual input from the nasal hemiretina of the right eye, and corresponded well to right peripheral phosphene sensation reported by the subjects. There was also activation in the bilateral secondary visual cortex (BA 18) and left association visual cortex (BA 19).

For RD subjects, TcES also activated a small region of anterior primary visual cortex (BA 17) in the left hemisphere (Fig. 5, bottom row, blue arrowhead). This region of activation was similar in location compared to the normal controls and corresponded to primary visual cortex that processes visual input from the peripheral nasal retina of the right eye. There was also bilateral activation in secondary visual cortex (BA 18) and activation of left association visual cortex (BA 19) near the parieto-occipital junction (Figs. 4 and 5).

In addition to visual cortex activation, significant activation was observed in bilateral frontal eye field (BA 8) and prefrontal cortices in both normal control and RD subjects. These cortical areas play a role in visual attention, fixation, and saccade (Anderson et al., 1994; de Haan et al., 2008). Activation was also seen in bilateral somatosensory cortex, primary and supplementary motor cortex, with stronger activity in the left hemisphere. Activation in these brain areas corresponded to physical sensation of ERG-Jet corneal electrode placed on the right eye during TcES and fine motor control exerted by the subjects to keep the electrode centered on the cornea.

### 3.6. Quantitative visual cortex comparisons

Quantitative PET imaging allowed us to compare changes in metabolic rate of glucose for each stimulation condition with baseline PET as the reference. Regions of interest were drawn to encompass primary visual cortex (BA 17)and secondary visual cortices (BA 18 and 19) in the subtraction PET image (stimulation minus baseline) for each subject. The average of all the voxels in each region of interest from each subject was used to calculate the overall average of each stimulation condition as shown in (Fig. 6). Statistically higher primary visual cortex (BA 17) activity was seen in normal controls than in RD subjects during both light stimulation ($p < 0.01$) and TcES ($p < 0.02$). During TcES, both primary visual cortex

(BA 17) and association visual cortex (BA 18 and 19) activation was higher in normal than RD subjects ($p < 0.02$). No statistically significant difference was observed between normal and RD subjects in secondary visual cortex (BA 18 and 19) activation during light stimulation.

## 4. Discussion

Light stimulation of the right eye in normal controls resulted in activation of primary (BA 17) and secondary visual cortex (BA 18 and 19) in both hemispheres. Primary visual cortex activation was found both above and below the calcarine sulcus at the occipital pole (Figs. 4 and 5). Similarly, light stimulation in the RD subjects activated primary visual cortex (BA 17) in the right occipital pole and association visual cortex (BA 18 and 19) on the left hemisphere. Compared to normal-sighted controls, a smaller region of activation in the primary visual cortex reached statistical significance in the RD group. This can be explained by differences in the extent and location of visual loss among the RD subjects.

The activation patterns measured in visual cortex during light stimulation from normal-sighted subjects are consistent with previous visual field mapping experiments. Using fMRI and a light stimulus, investigators have mapped the corresponding visual field to locations on the primary visual cortex (DeYoe et al., 1996; Engel et al., 1997; Sereno et al., 1995). They found that foveal representation was posteriorly located near the occipital pole of the primary visual cortex, while greater eccentricities were anteriorly represented. The temporal hemifield of each eye was represented on the ipsilateral hemisphere. Early PET studies that mapped visual cortex to light stimulation and visual attention demonstrated similar regions of brain activation as later confirmed with fMRI (Corbetta et al., 1991; Phelps et al., 1981). Since the light stimulus was a flashing square that subtended the central 10° field of view, our finding of occipital pole activation during light stimulation in normal-sighted subjects is consistent with central macular projection.

The bilateral activity in the association visual cortex could be explained on the basis of larger receptive fields subserved by these cortical regions compared to primary visual cortex. Observations made using fMRI indicated that in normal-sighted subjects the primary visual cortex was activated by a light stimulus projected to the contralateral visual field, whereas secondary visual cortex activation occurred bilaterally, with stronger activation on the contralateral visual cortex (Gonzalez et al., 2006). It may also be in part be related to visual attention as demonstrated by Kastner and Ungerleider (2001) who found significantly larger activation of V3 when the subject attended to visual stimulus when compared to looking but not attending to the visual stimulus. Our finding of greater left secondary visual cortex activation during central light stimulation of the right eye is consistent with these fMRI studies. A significant activation locus in the anterior primary visual cortex (BA 17) was found on the left hemisphere in normal controls (Fig. 5). This observation is consistent with findings from studies that looked at monocular photic eye stimulation in which the investigators attributed the phenomenon to nasal temporal asymmetry of photoreceptor and ganglion cell distribution (Miki et al., 2000; Toosy et al., 2001). A similar primary visual cortex activation locus was not found in the RD subjects.

The average phosphene threshold current for TcES using ERG-Jet corneal electrode was 0.72 ± 0.18 mA for the five normal-sighted controls and 3.08 ± 2.01 mA for the RD subjects. Miyake (Miyake et al., 1980) using a corneal contact electrode, found a threshold of 0.29 mA in healthy individuals at 5-ms pulse duration. Dorfman (Dorfman et al., 1987), using a Burian-Allen contact lens electrode, found thresholds between 2 and 3 mA at 1-ms pulse duration in four healthy individuals. Gekeler et al. (2006) reported an average threshold of 0.3 mA for healthy subjects using DTL electrode. Our average of 0.72 mA in normal-sighted controls at 2-ms pulse duration is comparable to their findings. The discrepancy may be attributed to differences in electrode type and methods used for threshold determination. For instance, Gekeler used psychophysical method, whereas Miyake and Dorfman used evoked cortical potential as a gauge for making threshold determination. Our average threshold current of 3.08 mA at 2-ms pulse duration is comparable to reported values of 4 mA at 4-ms pulse duration using Burian-Allen corneal electrode and 2.63 mA at 4-ms pulse duration using DTL electrode in patients with retinal degeneration (Gekeler et al., 2006). Although the method employed to obtain the threshold current has its drawback in its ability to account for potential experimenter bias in threshold determination; its subject-friendly expedience helps to minimize any confounding variable associated with discomfort from prolonged corneal electrode exposure. Furthermore, the precise determination of threshold current is not warranted for the overall PET study, since the stimulation current is set well above visual perception.

Transcorneal electrical stimulation with ERG-Jet electrode on the right eye resulted in phosphene sensation in the right (temporal) peripheral visual field in both the normal-sighted controls and RD subjects. The consistent phosphene percept in normal-sighted controls is corroborated by TcES modeling results which demonstrate preferential stimulation of retinal ganglion cell axon fibers along the peripheral nasal hemiretina of the right eye (Xie et al., 2011). The phosphene percepts described by RD subjects all fall in the same region of the visual field; however, the discrepancy in the shape and size of the phosphene may be attributed to remodeling of inner retinal layers. TcES resulted in retinotopically-matched primary visual cortex activation in the anterior calcarine corex on the left hemisphere (Fig. 5), which receives visual input from the nasal hemiretina of the right eye. This locus of anterior primary visual cortex activation was consistently seen in both normal and RD subjects, demonstrating that TcES stimulated a similar retinal region in the right eye. Based on the similarity in primary visual cortex activation between normal controls and RD subjects during TcES, it can be inferred that largescale remapping of the primary visual cortex has not occurred in the RD subjects as a result of visual deprivation. A recent study using fMRI has demonstrated similar absence of large-scale remapping of visual cortex in adult humans with congenital vision loss from juvenile macular degeneration (Baseler et al., 2011).

TcES in both normal-sighted and RD subjects activated bilateral association visual cortex (BA 18, 19) with stronger activation on the left hemisphere. Similar to light stimulation, the prominent activity in these areas may be explained on the basis of larger receptive fields and visual attention. We believe a similar effect was seen during TcES because the subjects were asked to pay attention to the phosphenes. Comparing the results from light stimulation and TcES in normal controls and RD subjects, the pattern of visual cortex activation is more

consistent between the two groups during TcES. This difference between the two groups can be largely explained in part by the variability of retinal locations stimulated during light stimulation in RD subjects and the consistent peripheral phosphene location elicited by TcES in the same RD subjects.

Quantitative comparison in the extent of activation during stimulation demonstrates significantly higher level of activation in the primary visual cortex (BA 17) of normal-sighted controls than RD subjects during both light stimulation and TcES (Fig. 6). Since the primary visual cortex is the main recipient of visual input from the retina, retinal degenerative processes will deprive the visual cortex of its primary input as reflected by a consistently lower amount of activation in RD subjects compared to normal controls. This relationship may be less direct on secondary and associated visual areas (BA 18 and 19) where feed forward and feedback loops add additional layers of complexity to visual processing.

In addition to visual cortex, increased activation was also observed in areas of prefrontal and orbitofrontal cortex, frontal eye field, and higher-order visual association areas, which have been shown to play a role in visual attention, fixation, and saccade (Anderson et al., 1994; de Haan et al., 2008).

There are limitations to this study, including a small sample size and the heterogeneous nature of retinal degeneration in the RD subject group. We attempted to minimize the heterogeneity by selecting RD subjects who have similar pattern of visual loss and share a comparable length of light-perception-only best visual acuity in hope that neural remodeling would be uniform and unbiased by the duration of visual loss. Despite dissimilar initial patterns of visual loss and different natural histories of progression amongst the RD subjects, the advanced stages of retinal degeneration have shown similar visual cortical response to retinal electrical stimulation. The design of the analysis takes into account the aggregate effect of stimulation condition across all subjects of the same group, thus minimizing individual variability in the comparison. Despite the limitations, we were able to achieve statistical significance in the functional imaging results. As a proof of concept, this study demonstrates the potential of using trans-corneal electrical stimulation as a promising method of assessing remodeling of retino-cortical pathway from visual loss; however, the spatial resolution of PET does not allow us to assess the effect of intra-retinal remodeling in the eyes of RD subjects. This technique can certainly be extended to fMRI in which multiple sets of functional images from a single individual can be acquired to enhance not only statistical significance and spatial resolution, but fine-tune the functional map tailored to each individual. Metallic coating and wires can introduce artifacts in fMRI images and may not be safely used in strong magnetic fields. New technologies such as carbon nanotube in combination with MRI-compatible coating that can render the electrode MRI-safe while maintaining its electrical conductive properties can be incorporated in fMRI studies of TcES. MRI-compatible deep brain stimulation electrodes, such as Ad-Tech depth electrodes, are commercially available for investigative treatment of epilepsy (Suthana et al., 2012). This technology can be extended to make corneal electrodes MRI-compatible. Since the location of the corneal electrode is far from the visual cortex, the hope is that any interference will be minimal. The current design of the ERG-Jet corneal electrode allows

one mode of TcES and one pattern of retinal activation. To further consolidate the validity of the results, it would be useful to stimulate different areas of the retina through manipulation of current flow via modified corneal electrode and stimulation parameters, and then compare the resulting primary visual cortex activation to the ret-inotopic map.

Based on our initial results, we expect both $^{18}$FDG-PET and fMRI to provide useful information for investigations of electrical stimulation of the retina. Specifically, functional imaging can reveal which brain areas are engaged by electrical stimulation of the retina. This will be important for understanding why some test subjects with retinal implant perform well, while others do not. We aim to extend the current study to look at functionality of retinal implant in vivo and incorporate fMRI in future studies.

## 5. Conclusion

This study demonstrates that electrical stimulation of the retina can activate the visual cortex and leads to visual perception in subjects with retinal degeneration. We have shown that TcES using ERG-Jet corneal electrode resulted in retinotopically-matched primary visual cortex activation in both normal-sighted and RD subjects. Patterns of early visual area activation between the two groups are more similar during TcES than light stimulation. Our findings suggest that primary visual cortex continues to maintain its retinotopy in RD subjects despite prolonged visual loss.

## Acknowledgements

*Funding/Support*: This research was supported in part by the US Department of Energy under grant DE-FC02-04ER63735, and in part by the National Science Foundation under grant CBET-0917458. We are especially grateful to Professor Rando Allik-mets for genotyping studies and members of the Division of Ophthalmic Imaging at the Edward S. Harkness Eye Institute of Columbia University Medical Center for their support.

## Abbreviations

| | |
|---|---|
| **BA** | Brodmann area |
| **$^{18}$FDG** | 2-deoxy-2-[$^{18}$F]fluoro-$_{D}$-glucose |
| **OCT** | optical coherence tomography |
| **PET** | positron emission tomography |
| **RD** | retinal degeneration |
| **RP** | retinitis pigmentosa |
| **TcES** | transcorneal electrical stimulation |

## References

Anderson TJ, Jenkins IH, Brooks DJ, et al. Cortical control of saccades and fixation in man. A PET study. Brain. 1994; 117:1073–1084.

Baker CI, Peli E, Knouf N, Kanwisher NG. Reorganization of visual processing in macular degeneration. J. Neurosci. 2005; 25:614–618. [PubMed: 15659597]

Baseler HA, Gouws A, Haak KV, et al. Large-scale remapping of visual cortex is absent in adult humans with macular degeneration. Nat. Neurosci. 2011; 14:649–655. [PubMed: 21441924]

Corbetta M, Miezin FM, Dobmeyer S, Shulman GL, Petersen SE. Selective and divided attention during visual discriminations of shape, color, and speed: functional anatomy by positron emission tomography. J. Neurosci. 1991; 11:2383–2402. [PubMed: 1869921]

de Haan B, Morgan PS, Rorden C. Covert orienting of attention and overt eye movements activate identical brain regions. Brain Res. 2008; 1204:102–111. [PubMed: 18329633]

DeYoe EA, Carman GJ, Bandettini P, et al. Mapping striate and extrastriate visual areas in human cerebral cortex. Proc. Natl. Acad. Sci. 1996; 93:2382–2386. [PubMed: 8637882]

Dilks DD, Baker CI, Peli E, Kanwisher N. Reorganization of visual processing in macular degeneration is not specific to the “preferred retinal locus”. J. Neurosci. 2009; 29:2768–2773. [PubMed: 19261872]

Dorfman LJ, Gaynon M, Ceranski J, Louis AA, Howard JE. Visual electrical evoked potentials: evaluation of ocular injuries. Neurology. 1987; 37:123–128. [PubMed: 3796828]

Engel SA, Glover GH, Wandell BA. Retinotopic organization in human visual cortex and the spatial precision of functional MRI. Cereb. Cortex. 1997; 7:181–192. [PubMed: 9087826]

Fujikado T, Morimoto T, Kanda H, et al. Evaluation of phosphenes elicited by extraocular stimulation in normals and by extraocular stimulation in normals and by suprachoroidal-transretinal stimulation in patients with reti-nitis pigmentosa. Graefe Arch. Clin. Exp. Ophthalmol. 2007; 245:1411–1419.

Gekeler F, Messias A, Ottinger M, et al. Phosphenes electrically evoked with DTL electrodes: a study in patients with retinitis pigmentosa, glaucoma, and homonymous visual field loss and normal subjects. Invest. Ophthalmol. Vis. Sci. 2006; 47:4966–4974. [PubMed: 17065515]

Gonzalez F, Relova JL, Prieto A, Peleteiro M, Romero MC. Hemifield dependence of responses to color in human fusiform gyrus. Vis. Res. 2006; 46:2499–2504. [PubMed: 16545857]

Hartong DT, Berson EL, Dryja TP. Retinitis pigmentosa. Lancet. 2006; 368:1795–1809. [PubMed: 17113430]

Humayun MS, de Juan EJ, Dagnelie G, et al. Visual perception elicited by electrical stimulation of retina in blind humans. Arch. Ophthalmol. 1996; 114:40–46. [PubMed: 8540849]

Humayun MS, Prince M, de Juan EJ, et al. Morphometric analysis of the extramacular retina from postmortem eyes with retinitis pigmentosa. Invest. Ophthalmol. Vis. Sci. 1999a; 40:143–148. [PubMed: 9888437]

Humayun MS, de Juan EJ, Weiland JD, et al. Pattern electrical stimulation of the human retina. Vis. Res. 1999b; 39:2569–2576. [PubMed: 10396625]

Kastner S, Ungerleider LG. The neural basis of biased competition in human visual cortex. Neuropsychologia. 2001; 39:1263–1276. [PubMed: 11566310]

Kawamura A. Study on characteristics of electrically evoked response (EER) in the rabbit eyes. J. Jpn. Ophthalmol. Soc. 1986; 90:1417–1421.

Marc RE, Jones BW. Retinal remodeling in inherited photoreceptor degenerations. Mol. Neurobiol. 2003; 28:139–147. [PubMed: 14576452]

Marc RE, Jones BW, Watt CB, Strettoi E. Neural remodeling in retinal degeneration. Prog. Retin. Eye Res. 2003; 22:607–655. [PubMed: 12892644]

Miki A, Liu GT, Raz J, et al. Contralateral monocular dominance in anterior visual cortex confirmed by functional magnetic resonance imaging. Am. J. Ophthalmol. 2000; 130:821–824. [PubMed: 11124303]

Miyake Y, Yanagida K, Yagasaki K. Clinical application of EER (electrically evoked response). (1) Analysis of EER in normal subjects. Nihon Ganka Gakkai Zasshi. 1980; 84:354–360. [PubMed: 7395667]

Morimoto T, Fukui T, Matsushita K, et al. Evaluation of residual retinal function by papillary constrictions and phosphenes using transcorneal electrical stimulation in patients with retinal degeneration. Graefe Arch. Clin. Exp. Ophthalmol. 2006; 244:1283–1292.

Phelps ME, Kuhl DE, Mazziotta JC. Metabolic mapping of the brain’s response to visual stimulation: studies in humans. Science. 1981; 211:1445–1448. [PubMed: 6970412]

Potts AM, Inoue J. The electrically evoked response (EER) II. Effect of adaptation and retinitis pigmentosa. Invest. Ophthalmol. 1969; 8:605–612. [PubMed: 5359577]

Potts AM, Inoue J. The electrically evoked response of the visual system (EER) III. Further consideration to the origin of the EER. Invest. Ophthalmol. 1970; 9:814–819. [PubMed: 5479448]

Potts AM, Inoue J, Buffum D. The electrically evoked response of the visual system (EER). Invest. Ophthalmol. Vis. Sci. 1968; 7:269–278.

Rizzo JF, Wyatt J, Loewenstein J, Kelly S, Shire D, Wyatt J. Methods and perceptual thresholds for short-term electrical stimulation of human retina with microelectrode arrays. Invest. Ophthalmol. Vis. Sci. 2003; 44:5355–5361. [PubMed: 14638738]

Rombouts SA, Barkhof F, Sprenger M, Valk J, Scheltens P. The functional basis of ocular dominance: functional MRI (fMRI) finding. Neurosci. Lett. 1996; 221:1–4. [PubMed: 9014166]

Santos A, Humayun MS, de Juan EJ, et al. Preservation of the inner retina in retinitis pigmentosa. A morphometric analysis. Arch. Ophthalmol. 1997; 115:511–515.

Sereno MI, Dale AM, Reppas JB, et al. Borders of multiple visual areas in humans revealed by functional magnetic resonance imaging. Science. 1995; 268:889–893. [PubMed: 7754376]

Sharma RK, Ehinger B. Management of hereditary retinal degenerations: present status and future directions. Surv. Ophthalmol. 1999; 43:427–444. [PubMed: 10340561]

Shimazu K, Miyaki Y, Watanabe S. Retinal ganglion cell response properties in the transcorneal electrically evoked response of the visual system. Vis. Res. 1999; 39:2251–2260. [PubMed: 10343806]

Stone JL, Barlow WE, Humayun MS, et al. Morphometric analysis of macular photoreceptors and ganglion cells in retinas with retinitis pigmentosa. Arch. Ophthalmol. 1992; 110:1634–1639. [PubMed: 1444925]

Suthana N, Haneef Z, Stern J, et al. Memory enhancement and deep-brain stimulation of the entorhinal area. N. Engl. J. Med. 2012; 366:502–510. [PubMed: 22316444]

Takei K. Localization of the components of the electrically evoked response (EER) of the visual system. Nihon Ganka Gakkai Zasshi. 1988; 92:1682–1686. [PubMed: 3213771]

Toosy AT, Werring DJ, Plant GT, Bullmore ET, Miller DH, Thompson AJ. Asymmetrical activation of human visual cortex demonstrated by functional MRI with monocular stimulation. Neuroimage. 2001; 14:632–641. [PubMed: 11506536]

Wang GJ, Volkow ND, Roque CT, et al. Functional importance of ventricular enlargement and cortical atrophy in healthy subjects and alcoholics as assessed with PET, MR imaging, and neuropsychologic testing. Radiology. 1993; 186:59–65. [PubMed: 8416587]

Xie J, Wang GJ, Yow L, et al. Modeling and percept of transcorneal electrical stimulation in humans. IEEE Trans. Biomed. Eng. 2011; 58:1932–1939. [PubMed: 20952323]

Yanai D, Lakhanpal RR, Weiland JD, et al. The value of preoperative tests in the selection of blind patients for a permanent microelectronic implant. Trans. Am. Ophthalmol. Soc. 2003; 101:223–228. [PubMed: 14971581]

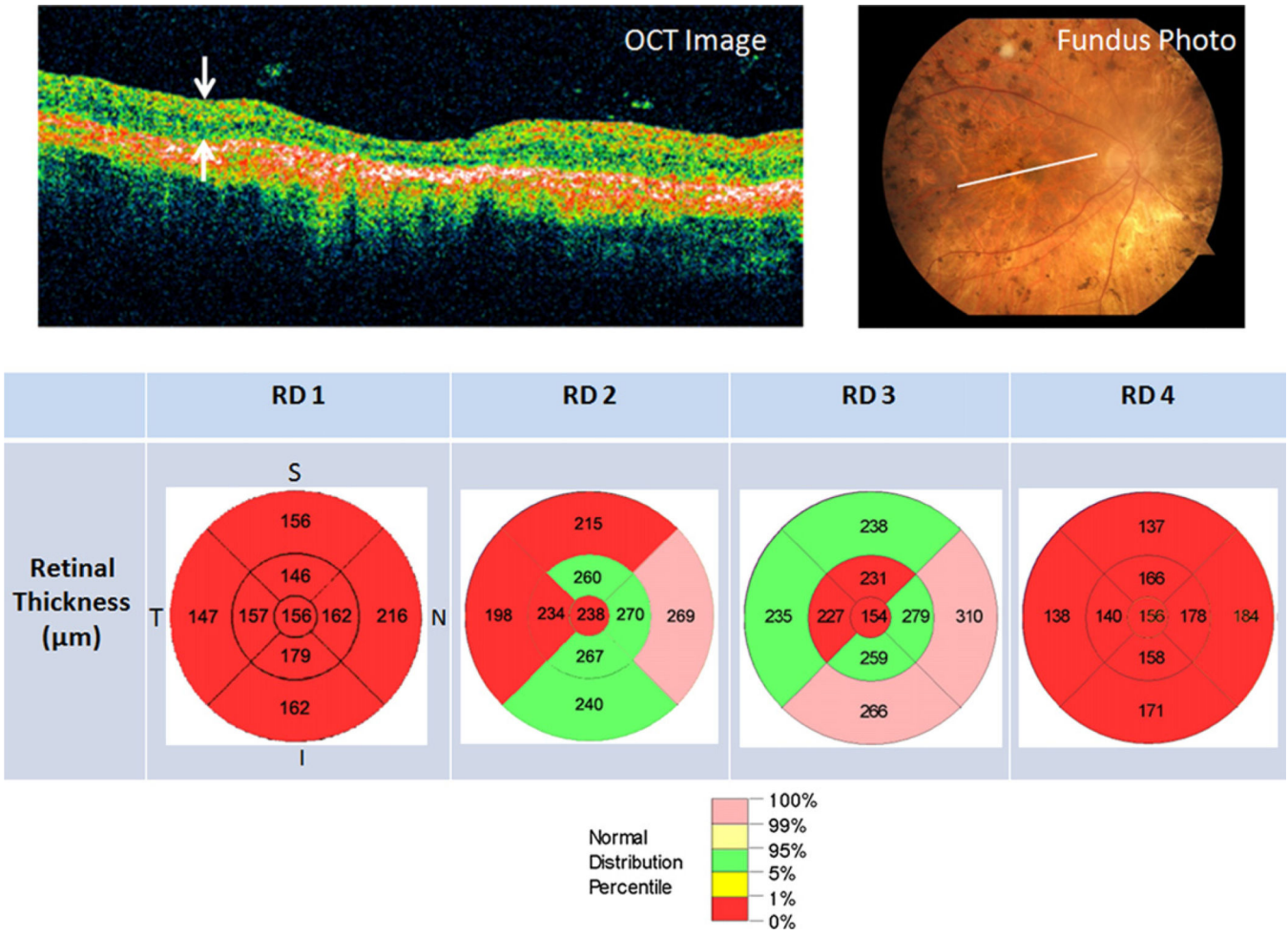


**Fig. 1.**

Optical coherence tomography (OCT) study of retinal degeneration (RD) subjects' right eye. (Top left) OCT raster image through the macula delineated by the white line in the corresponding color fundus photograph for RD 3 (Top right). (Top left) White arrows enclose the retinal layer. (Bottom) Retinal thickness plots indicate retinal thickness in micrometer by quadrant and eccentricity. Color coding corresponds to normal distribution percentile with red denoting below 1% normal distribution for the corresponding retinal thickness. I: inferior; N: nasal; S: superior; T: temporal.


**Fig. 2.**

Neurostimulator setup for TcES. Digitimer train generator (DG2A) generates the pulse triggers for the Digitimer DS7A neurostimulator which in turn outputs alternating polarity current pulses to the ERG-Jet electrode (photograph courtesy of Fabrinal SA).

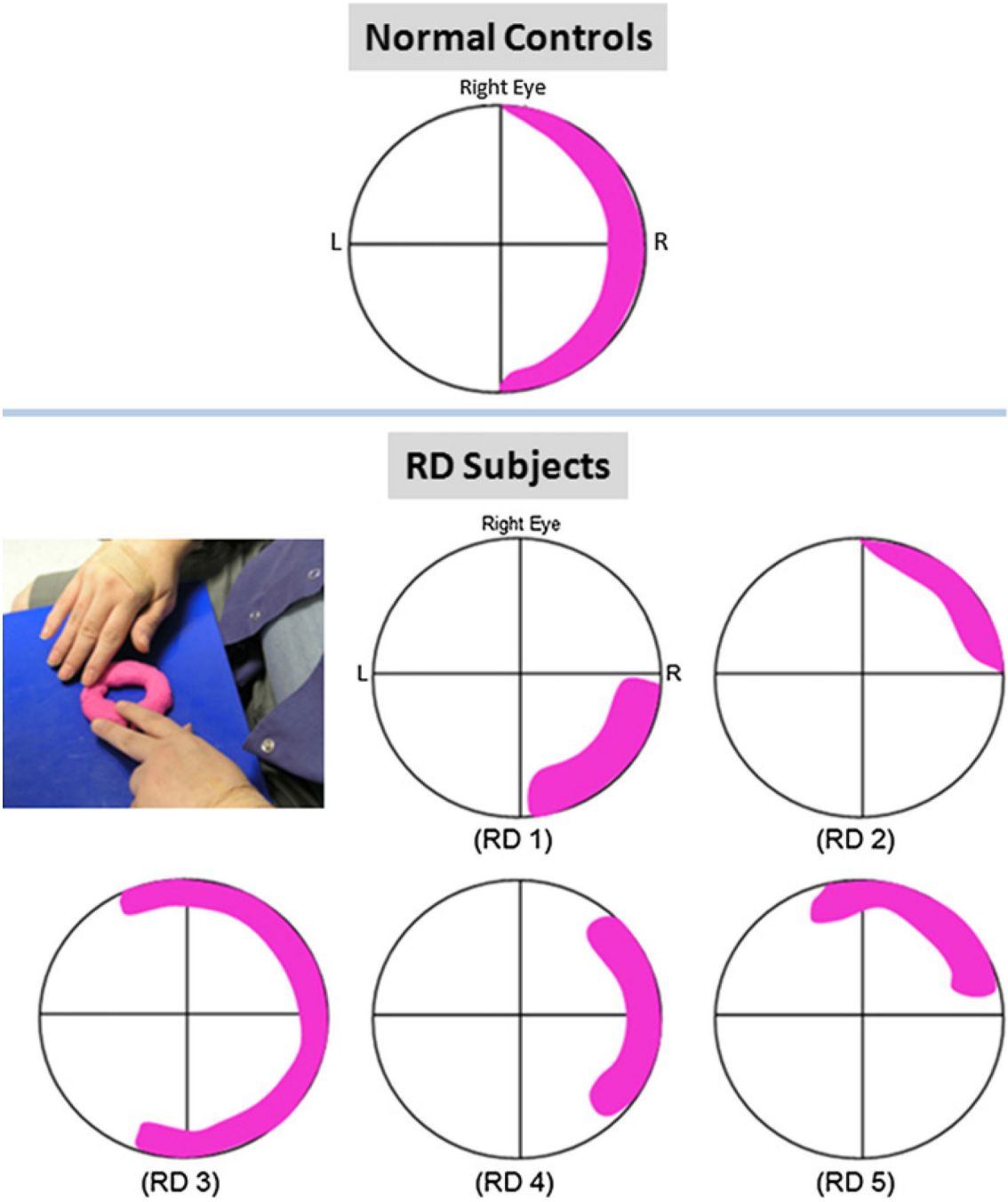


**Fig. 3.**

Phosphene sensation during transcorneal electrical stimulation. Pink overlay on the visual field grid indicates location and shape of phosphene reported by the subjects. (Top) cresent-shaped phosphene reported by all five normal controls; (Middle and bottom rows) phosphene sensation reported by the five retinal degenerative subjects; (Left, middle row) photograph of one retinal degenerative subject describing phosphene sensation using Play-Doh.

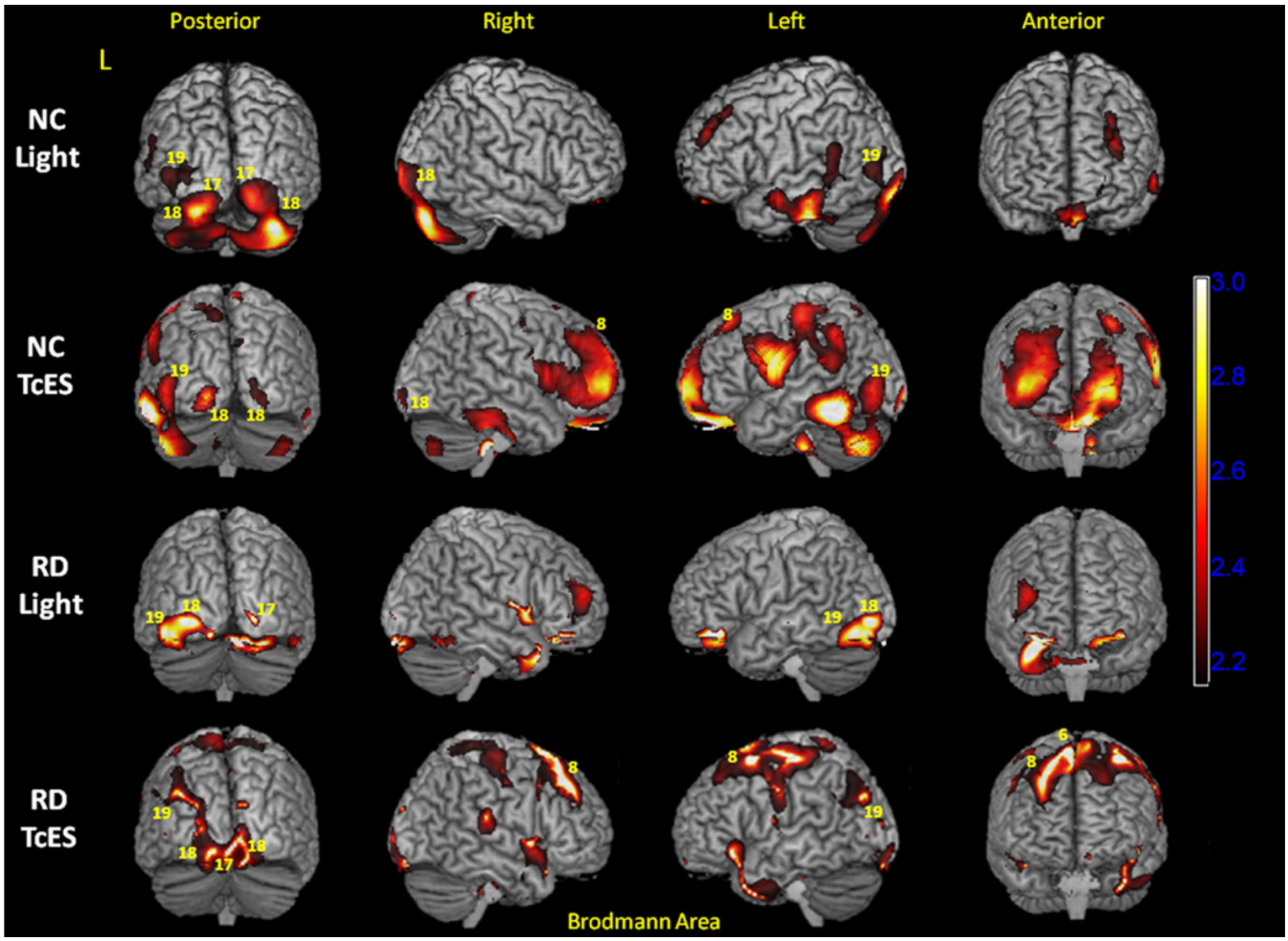


**Fig. 4.**

3-D statistical parametric map (SPM) projection of light stimulation and transcorneal electrical stimulation (TcES) activation. (Top row) Increase in cortical PET FDG activity compared to baseline ($p < 0.05$) during light stimulation in normal controls; (Second row) TcES in normal controls; (Third row) light stimulation in retinal degenerative subjects; and (Bottom row) TcES in retinal degenerative subjects. SPM maps are overlaid on top of rendered 3-D MRI brain surfaces. Selected Brodmann areas that exhibit increased activity during stimulation conditions are labeled as yellow numeric values. Scale bar = t-value. L: left hemisphere; NC: normal controls; RD: retinal degenerative subjective.

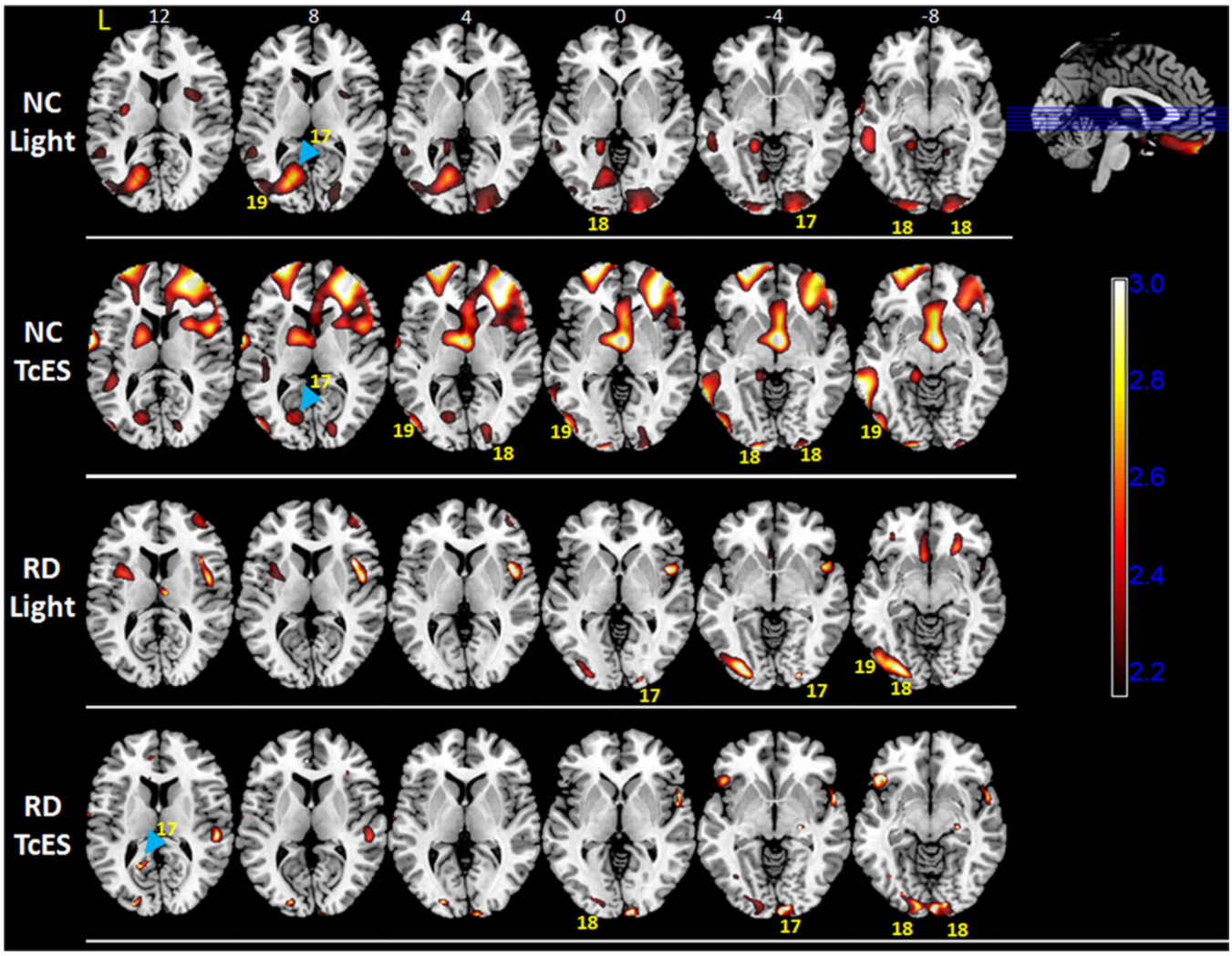


**Fig. 5.**

Statistical parametric maps for normal controls and retinal degenerative subjects overlaid on transverse MRI template, (Top row) showing areas of increased PET FDG brain activity compared to baseline ($p < 0.05$) during light stimulation in normal controls, (Second row) during transcorneal electrical stimulation (TcES) in normal controls, (Third row) during light stimulation in RD subjects, and (Bottom row) during TcES in RD subjects. Numerals above the top row of MRI transverse sections denote position in millimeter above ($z > 0$) and below ($z < 0$) the plane transecting the anterior and posterior commissures ($z = 0$). Selected Brodmann areas are labeled as yellow numeric values. Scale bar = t-value. L: left hemisphere; NC: normal controls; RD: retinal degenerative.

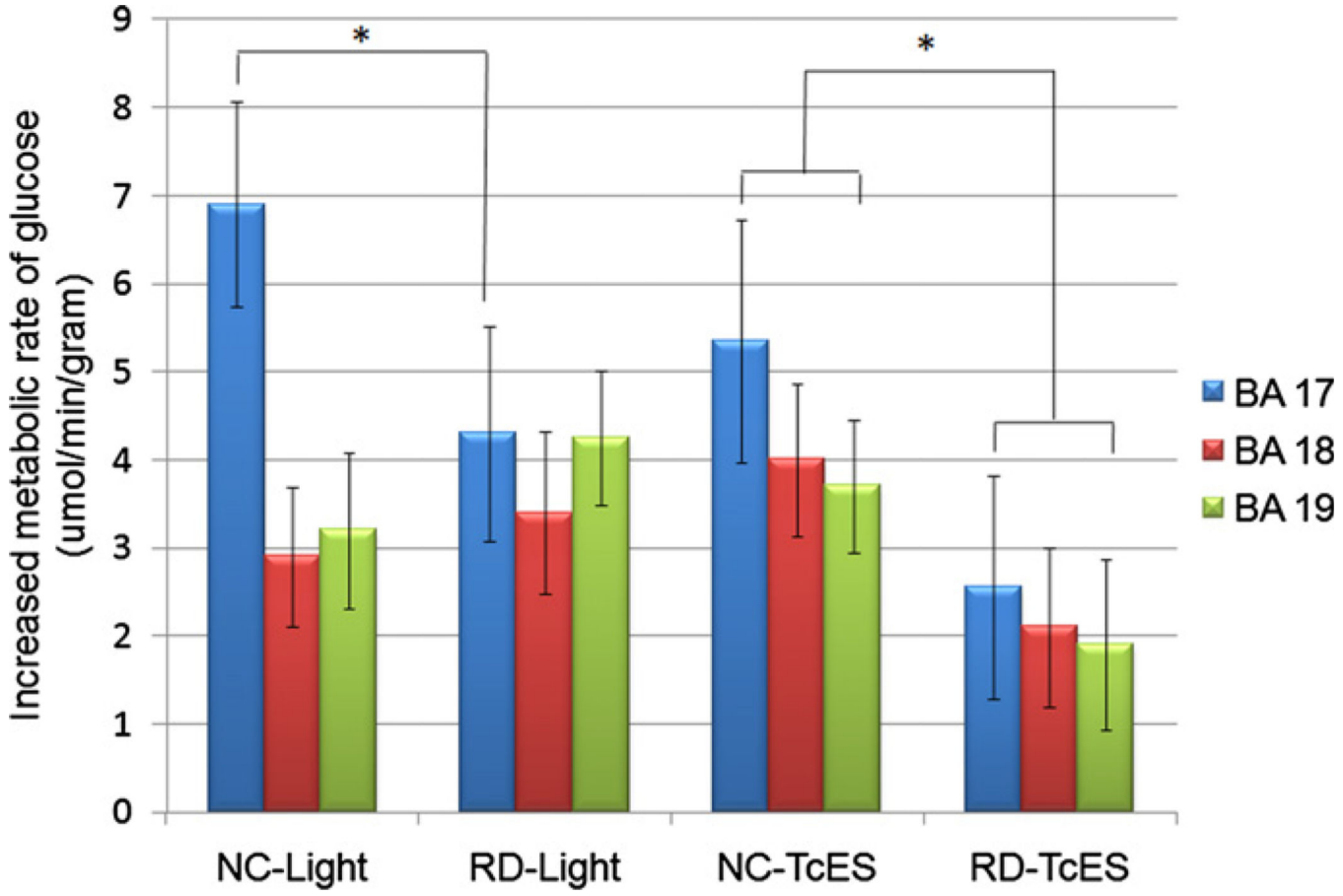


**Fig. 6.**

Quantitative PET comparison of primary and secondary visual cortex between normal controls and retinal degenerative subjects. Vertical axis represents increases in metabolic rate of glucose compared to baseline, in units of μmol of FDG consumed per minute per gram of brain tissue. BA: Brodmann area; NC: normal controls; RD: retinal degenerative subjects; error bar represents standard deviation; * denotes statistically significant difference between respective columns marked by brackets, $p < 0.05$.

**Table 1**

Normal control and retinal degenerative subjects identifying data.

| ID Index | Age (yr) | Gender | Clinical Diagnosis | Age of RD Onset (yr) | Mutation | Visual Acuity | Family History | ERG-Jet Threshold (mA) |
|---|---|---|---|---|---|---|---|---|
| NC 1 | 47.5 | F | n/a | n/a | n/a | n/a | n/a | 0.55 |
| NC 2 | 27.0 | M | n/a | n/a | n/a | n/a | n/a | 0.80 |
| NC 3 | 24.0 | M | n/a | n/a | n/a | n/a | n/a | 0.60 |
| NC 4 | 41.8 | F | n/a | n/a | n/a | n/a | n/a | 1.00 |
| NC 5 | 31.4 | M | n/a | n/a | n/a | n/a | n/a | 0.65 |
| RD 1 | 42.1 | F | Leber's congenital amaurosis (LCA) | 14 | CRX[a] | OU light perception | Relative with AMD & LCA | 4.5 |
| RD 2 | 32.0 | M | Bull's eye cone-rod dystrophy Stargardt (Group 3) | 4 | ABCA4 G1725 | OU finger counting up to 1 ft | No family history | 1.6 |
| RD 3 | 56.7 | M | Retinitis pigmentosa | 14 | Not found[b] | OU light perception | No family history | 2.5 |
| RD 4 | 52.2 | M | Retinitis pigmentosa | 20 | Not found[b] | OU light perception | No family history | 5.8 |
| RD 5 | 35.7 | M | Retinitis pigmentosa | 4 | Not found[b] | OU light perception | No family history | 1.0 |

AMD: age-related macular degeneration; F: female; LCA: Leber's congenital amaurosis; M: male; NC: normal control; RD: retinal degenerative subject; OU: both eyes.

[a] Novel, non-published CRX mutation.

[b] Non-published, de novo mutation basedongene screening for CERKL, CNGB1, MERTK, PDE6B, PNR, RDH12, RGR, RLBP1, SAG, TULP1, CRB, RPE65, USH3A, LRAT, and PROM1 (ARRPgenetest, Asper Ophthalmics, Tartu, Estonia).